Published in final edited form as:
J Control Release. 2017 September 10; 261: 105–112. doi:10.1016/j.jconrel.2017.06.022.

Sonic-Hedgehog pathway inhibition normalizes desmoplastic tumor microenvironment to improve chemo- and nanotherapy

Fotios Mpekris[#1], **Panagiotis Papageorgis**[#1,2], **Christiana Polydorou**[#1], **Chrysovalantis Voutouri**[1], **Maria Kalli**[1], **Athanassios P. Pirentis**[1], and **Triantafyllos Stylianopoulos**[1,*]

[1]Cancer Biophysics Laboratory, Department of Mechanical and Manufacturing Engineering, University of Cyprus, Nicosia, Cyprus

[2]Department of Life Sciences, Program in Biological Sciences, European University Cyprus, Nicosia, Cyprus

[#] These authors contributed equally to this work.

Abstract

Targeting the rich extracellular matrix of desmoplastic tumors has been successfully shown to normalize collagen and hyaluronan levels and re-engineer intratumoral mechanical forces, improving tumor perfusion and chemotherapy. As far as targeting the abundant cancer-associated fibroblasts (CAFs) in desmoplastic tumors is concerned, while both pharmacologic inhibition of the sonic-hedgehog pathway and genetic depletion of fibroblasts have been employed in pancreatic cancers, the results between the two methods have been contradictory. In this study, we employed vismodegib to inhibit the sonic-hedgehog pathway with the aim to i) elucidate the mechanism of how CAFs depletion improves drug delivery, ii) extent and evaluate the potential use of sonic-hedgehog inhibitors to breast cancers, and iii) investigate whether sonic-hedgehog inhibition improves not only chemotherapy, but also the efficacy of the most commonly used breast cancer nanomedicines, namely Abraxane® and Doxil®. We found that treatment with vismodegib normalizes the tumor microenvironment by reducing the proliferative CAFs and in cases the levels of collagen and hyaluronan. These modulations re-engineered the solid and fluid stresses in the tumors, improving blood vessel functionality. As a result, the delivery and efficacy of chemotherapy was improved in two models of pancreatic cancer. Additionally, vismodegib treatment significantly improved the efficacy of both Abraxane and Doxil in xenograft breast tumors. Our results suggest the use of vismodegib, and sonic hedgehog inhibitors in general, to enhance cancer chemo- and nanotherapy.

Keywords

re-engineering cancer; tumor microenvironment; tumor perfusion; drug delivery; pancreatic cancer; breast cancer

[*]Address correspondence To: Triantafyllos Stylianopoulos,Ph.D., Cancer Biophysics Laboratory, Department of Mechanical and Manufacturing Engineering, University of Cyprus, P.O. Box 20537, Nicosia, 1678, Cyprus, tel: +357 2289 2238, fax: +357 2289 5081, tstylian@ucy.ac.cy.

Europe PMC Funders Author Manuscripts

1 Introduction

Inefficient delivery of cytotoxic drugs to solid tumors can dramatically reduce the efficacy of chemotherapy and nanotherapy and thus, negatively affect the quality of life and survival of cancer patients. This can explain in large part why standard therapies many times fail to treat desmoplastic cancers, i.e., tumors abnormally rich in stromal components such as breast and pancreatic cancers, even though these agents are potent enough to eradicate cancer cells in *in vitro* systems. Effective delivery of drugs to solid tumors is hindered by abnormalities in the structure of the tumor vasculature, which can drastically reduce tumor perfusion and as a result the systemic delivery of the drug [1, 2].

In desmoplastic tumors, in particular, mechanical interactions among rapidly proliferating cancer cells, cancer associated fibroblasts (CAFs), extracellular matrix (ECM) fibers, primarily collagen and hyaluronan, and the surrounding normal tissue lead to accumulation of intratumoral solid stresses, causing vessel compression and hypo-perfusion [2–6]. To improve blood vessel functionality and treatment efficacy, already approved drugs with anti-fibrotic properties have been repurposed (e.g., losartan, tranilast, pirfenidone) and it has been shown that these drugs can normalize the microenvironment of breast and pancreatic tumors to improve the delivery of chemotherapy and nanomedicine [7–9]. Importantly, this strategy has already reached clinical trials (clinicaltrials.gov identifier: NCT01821729) and the first results of a phase-II trial for the use of losartan to enhance therapy in pancreatic cancer patients confirm the preclinical findings [10].

Apart from the use of anti-fibrotic drugs, pertinent studies have employed inhibitors of the Sonic Hedgehog (SHH) signaling pathway to achieve pharmacologic depletion of CAFs in pancreatic cancers. Inhibition of SHH signaling using saridegib was shown to reduce proliferation and number of CAFs in mouse models of pancreatic cancer, improve blood vessel functionality and eventually the efficacy of gemcitabine [11]. Despite these encouraging data, however, saridegib failed in a phase-II clinical trial for previously untreated patients with metastatic pancreatic cancer when combined with gemcitabine [12]. Similarly, more recent phase-II clinical trials in an unselected cohort of patients with metastatic pancreatic cancer indicated that, while modestly improved, combination of vismodegib and gemcitabine did not result in a statistically significant increase in overall survival compared to gemcitabine alone [13]. However, these results could be due to different reasons, such as intrinsic resistance to gemcitabine as increased delivery of a drug might not benefit patients if cancer cells are or become resistant to that drug, or these cancers are already at such an advanced stage for survival improvement to be significantly demonstrated. Moreover, random selection of patients could also affect clinical trial results, since one would expect vismodegib to be particularly beneficial for highly desmoplastic, fibroblast-rich pancreatic tumors.

Additionally, a series of recent *in vivo* studies have shown that deletion of CAFs by genetic manipulation in mouse models induces immunosuppression and promotes tumour progression in pancreatic cancers [14, 15]. Therefore manipulation of CAFs has been shown to both promote and restrain tumor progression, but any comparison between genetic

deletion and pharmacologic depletion should be viewed with caution and take into account that these methods significantly differ from each other as:

- **i.** Genetic deletion is chronic and effects of genetic deletion are not reversible. On the other hand, pharmacologic depletion is acute and effects are reversible when the treatment stops.
- **ii.** Pharmacological agents could be delivered specifically to the tumor site while genetic deletion might affect the entire body.
- **iii.** Genetic deletion might improve drug delivery and increase hypoxia, whereas pharmacologic depletion improves drug delivery and decreases hypoxia.

In this study, we revisited the use of SHH inhibitors to target CAFs with the aim to i) elucidate the mechanism of how CAFs depletion improves drug delivery, ii) extent and evaluate the potential use of SHH inhibitors to breast cancers, and iii) investigate whether SHH inhibition can improve not only chemotherapy, but also the efficacy of the most commonly used breast cancer nanomedicines, namely Abraxane® and Doxil®. To achieve our aims, we employed vismodegib (Erivedge®) in mouse tumor models for pancreatic and breast cancers to explore its ability to normalize the tumor microenvironment, decrease solid stress levels and improve tumor perfusion and therapeutic outcomes.

Vismodegib is the first oral medication approved by the US Food and Drug Administration in 2012 for adults with metastatic or locally advanced Basal Cell Carcinoma that has recurred after surgery or for patients who are not candidates for surgery or radiation. Previous studies have shown that administration of vismodegib in a mouse model of medulloblastoma and in xenograft models of primary human tumors, including colorectal and pancreatic carcinoma, inhibits SHH pathway and exerts antitumor activity [16–19].

To elucidate the mechanism by which depletion of CAFs improves drug delivery, we initially hypothesized that depleting stromal cells in primary pancreatic tumors will reduce solid stresses and improved the functionality of tumor blood vessels. To investigate this, we employed two human pancreatic cancer cell lines, namely MiaPaCa2 and BxPC3 to develop xenograft tumor models in immunodeficient mice. We show that vismodegib reduces solid stresses, decreases interstitial fluid pressure (IFP), improves perfusion, increases delivery of chemotherapy and improves therapeutic outcomes. Furthermore, we show that these observations are not only due to the reduction in the activity of CAFs but also due to the decrease in collagen and hyaluronan tumor content due to SHH signaling pathway inhibition and downregulation of downstream key effector genes Gli1 and Gli2. Finally, we developed an orthotopic xenograft breast tumor model, using the human breast cancer cell line MCF10CA1a, to study the effect of combining vismodegib with two clinically approved nanoparticles of different sizes, Abraxane (10 nm) and Doxil (100 nm), and show that vismodegib can also enhance the efficacy of these common cancer nanomedicines.

2 Materials and Methods

2.1 Cell culture

MiaPaCa2 human pancreatic cancer cell line and BxPC3 human primary pancreatic adenocarcinoma cell line were purchased from ATCC and were maintained in Dulbecco's Modified Eagle Medium (DMEM) supplemented with 10% Fetal Bovine Serum (FBS) and 1% antibiotics. MCF10CA1a human breast cancer cell line was obtained from the Karmanos Cancer Institute (Detroit, MI, USA) and maintained as previously described [20].

2.2 Drugs and reagents

Vismodegib (GDC-0449, Erivedge) was purchased from Selleckchem and the compound was formulated in a 10 mg/mL suspension in MCT (0.5% methylcellulose, 0.2% Tween 80), as previously described [16]. Gemzar (Gemcitabine, Lilly) was dissolved in 0.9% NaCl (12.5 mg/ml stock). Doxil (Pegylated liposomal doxorubicin, Janssen Pharmaceuticals) was purchased as already made solution (2 mg/ml) and Abraxane (Albumin-bound paclitaxel, Celgene) was solubilized in 0.9% NaCl in final stock concentration of 5 mg/ml.

2.3 Animal tumor models and treatment protocols

Xenograft pancreatic tumor models were generated by subcutaneous implantation of 2×10^6 MiaPaCa2 or BxPC3 cells resuspended in 40 μl of serum-free medium into 6-week old male NOD/SCID mice. Vismodegib was administered orally once a day at different doses (40mg/Kg or 100mg/Kg, as indicated) from day 35 in MiaPaCa2 and day 4 in BxPC3 post-implantation, 10 days before the initiation of chemotherapy. Gemcitabine (50 mg/kg) was administered by intraperitoneal (i.p.) injection when tumors reached an average size of ~200 mm^3; from day 45 in MiaPaCa2 and day 13 in BxPC3 post-implantation, every 72 hours. Orthotopic xenograft breast tumors were generated by implantation of 5×10^5 MCF10CA1a cells resuspended in 40 μl of serum-free medium into the mammary fat pad of 6-week old female CD1 nude immunodeficient mice. Vismodegib (40 mg/kg) was administered orally from day 4 post-implantation. In both models, Doxil (3mg/kg) and Abraxane (20 mg/kg) were administered by intravenous (i.v.) injections on day 14 and 21 post-implantation [8, 21–23]. During the course of each experiment, tumor growth was monitored daily and the planar dimensions (x, y) were measured using a digital caliper. Tumor volume was calculated using the volume of an ellipsoid and assuming that the third dimension, z, is equal to $\sqrt{xy}$. All *in vivo* experiments were conducted in accordance with the animal welfare regulations and guidelines of the Republic of Cyprus and the European Union under a license acquired by the Cyprus Veterinary Services (No CY/EXP/PR.L1/2014), the Cyprus national authority for monitoring animal research.

To study alterations in the tumor microenvironment, right before the end of each treatment protocol, animals were anesthetized by i.p. injection of Avertin (200mg/kg) and interstitial fluid pressure was measure using the wick-in-needle technique [3, 24, 25]. Next, mice were injected intracardially with 100μl biotinylated lectin (1mg/ml, Vector Labs), which was allowed to distribute throughout the body for 7 minutes [7–9]. Finally, mice were sacrificed via CO2 inhalation and tumors were excised for measurement of mechanical properties and/or histological analysis.

2.4 Fluorescent immunohistochemistry and vessel perfusion histology

MiaPaCa2 and BxPC3 pancreatic tumors were excised from mice, fixed in 4% paraformaldehyde, dehydrated through an ethanol series and embedded in paraffin wax before sectioning (7-mm thickness). Hematoxylin and eosin (H&E) and Masson's trichrome staining were performed using previously described methods [11, 20]. For immunofluorescence analysis, samples were embedded in optimal cutting temperature compound (OCT) upon tumor excision. Transverse 40μm-thick tumor sections were made using the Tissue-Tek Cryo3 (SAKURA) and immunostained using antibodies against collagen I (ab34710), CD31 (BD553370) and hyaluronan (ab53842) and then detected using appropriate secondary fluorescent antibodies. For alpha-smooth muscle actin (a-SMA) (ab7817) and Ki67 (ab15580) staining, tumors were fixed in 4% paraformaldehyde and embedded in paraffin before sectioning, as previously described [8, 11, 20].

For blood vessel perfusion analysis, mice were slowly injected with 100 μl of 1 mg/ml biotinylated lycopersicon esculentum (tomato) lectin (Vector Labs) via intracardiac injection 7 minutes prior to euthanization and tumor removal. Upon excision, tumors were fixed in 4% paraformaldehyde, embedded in OCT and frozen. Transverse 40 μm-thick tumor sections were produced and stained with an antibody CD31. Streptavidin-conjugated and fluorescently-labeled secondary antibodies against lectin and CD31 were used to detect these antigens, respectively.

Images from anti-collagen I, anti-CD31, anti-hyaluronan and anti-biotin-stained sections were analyzed based on the area fraction of positive staining. To avoid any bias, the analysis was performed automatically using a previously developed in-house code in MATLAB (MathWorks, Inc., Natick, MA, USA) [3]. Images from five different sections per tumor (from the interior and the periphery) were taken using an Olympus BX53 fluorescent microscope at ×10 magnification and were analyzed by keeping the analysis settings and thresholds identical for all tumors.

2.5 Biodistribution analysis

For biodistribution analysis, 20mg/kg Doxorubicin (Actavis) was injected intravenously in control or vismodegib-treated animals and 4 hours post-injection they were sacrificed. Seven animals per group were tested (n=7). The tumors and respective tissues were excised from the mice and were stored at -80 °C until extraction and further analysis. For doxorubicin extraction from tumors and tissues, a previously described method was used [8, 9, 26]. Doxorubicin concentration in tissue sample homogenates was determined by quantification of fluorescence intensity (Ex.: 470 nm, Em: 590 nm).

2.6 RNA isolation, cDNA synthesis, and real-time polymerase chain reaction

Total RNA was isolated from pancreatic tumors using standard Qiazol-based protocol (Qiagen) and cDNA synthesis was performed using reverse transcriptase III (RT-III) enzyme and random hexamers (Invitrogen). Real-time polymerase chain reaction (PCR) was performed using Sybr Fast Universal Master Mix (Kapa) and calculation of changes in gene expression between compared groups was performed using the ΔΔCt method, as previously described [27]. Mouse-specific primers were used for gene expression analysis in stromal

cells from MiaPaCa2 and BxPC3 tumors, while human-specific primers were used for gene expression analysis in MiaPaCa2 and BxPC3 cancer cells in tumors (Supplementary Table 1). All reactions were performed using a CFX-96 real-time PCR detection system (Biorad) under the following conditions: 95°C for 2 min, 95°C for 2 sec, 60°C for 20 sec, 60°C for 1 sec, steps 2-4 for 39 cycles.

2.7 Mechanical testing measurements for calculation of elastic modulus and hydraulic conductivity

The elastic modulus was calculated using an unconfined compression experimental protocol. Following tumor excision, tumor specimens 3×3×2 mm (length × width × thickness) were loaded on a high precision mechanical testing system (Instron, 5944, Norwood, MA, USA) and compressed to a final strain of 30% with a strain rate of 0.05mm/min. The elastic modulus was calculated from the slope of the stress-strain curve.

For the calculation of the hydraulic conductivity stress relaxation experiments were performed in compression. Specimens underwent four cycles of testing for each of which a 5% compressive strain was applied for 1 minute, followed by a 10-minute hold. Subsequently, The hydraulic conductivity was calculated by fitting a mathematical biphasic model of soft tissue mechanics [28, 29] to the experimental data, as previously described [8, 9].

3 Results

3.1 Vismodegib reduces functionality of CAFs *in vivo*

First, to validate that vismodegib targets CAFs *in vivo*, mice bearing MiaPaCa2 and BxPC3 tumors were treated with 40 mg/kg vismodegib. Animals orally received vismodegib on a daily basis starting 35 days (MiaPaCa2) or 4 days (BxPC3) post-implantation of cancer cells, for a period of 25 days or 23 days, respectively, according to previous studies [16, 17, 30–33]. Upon tumor excision, co-immunofluorescence analysis was performed on tumor sections to detect alpha-smooth muscle actin (a-SMA), as a CAF's marker, and Ki-67 to identify the proliferating cells. Then, the tumor area fraction in which a-SMA and Ki-67 staining overlapped (a-SMA/Ki67 positive cells) was quantified and compared between the two groups, to detect the presence of actively proliferating CAFs (Figure 1A) [11]. We found that vismodegib significantly reduced the fraction of proliferating CAFs *in vivo* (Figure 1B). Fraction of proliferating CAFs as a function of total a-SMA are presented in Supplementary Figure S1. Furthermore, H&E as well as Masson’s trichrome staining of MiaPaCa2 and BxPC3 tumor sections indicated that vismodegib treatment resulted in a more sparse cell network and decreased collagen fibers compared to controls, presumably due to the reduction in the number of CAFs (Supplementary Figure S2) as previously reported [11, 34].

3.2 Vismodegib remodels the tumor ECM by reducing collagen and hyaluronan levels

Additionally, it is possible that vismodegib could also indirectly reduce tumor ECM content through inhibition of CAFs and suppression of collagen and hyaluronan synthesis. To determine the effect of vismodegib on tumor ECM components, we performed immunofluorescence analysis of tumor cryosections followed by area fraction quantification.

We found that vismodegib treatment decreased collagen content in MiaPaCa2 by 20%, whereas no change was observed in BxPC3 tumors (Figure 2A, 2E), which could be attributed to differences in the genetic background of these cells. On the other hand, area fraction quantification indicated that hyaluronan levels were decreased in both MiaPaCa2 and BxPC3 tumors by 23% and 32%, respectively, compared to control-treated tumors (Figure 2B, 2F). Similar effects on collagen and hyaluronan levels were observed when MiaPaCa2 tumors received a higher dose of vismodegib (100 mg/kg) (Supplementary Figure S3).

Subsequently, we investigated the effect of vismodegib on the functionality of tumor blood vessels. We measured the percentage of perfused blood vessels of the control and vismodegib-treated tumors by staining tissue cryosections with antibodies against the endothelial marker CD31 and biotinylated lectin, which marks the functional tumor vessels. The fraction of perfused vessels was calculated based on the ratio of the area of biotinylated lectin positive (+) to the CD31 positive (+) vessels. We found that in vismodegib-treated mice the fraction of perfused vessels was significantly increased in both MiaPaCa2 and BxPC3 tumors by approximately 2.5-fold and 50%, respectively, compared to controls (Figure 2G). Furthermore, the total area of vessels (CD31+ area) in both pancreatic tumor models remained unaffected (Figure 2H). Similar results on perfused vessels as well the total number of vessels were obtained when MiaPaCa2 tumors received 100 mg/kg vismodegib (Supplementary Figure S3). Overall, our data suggest that vismodegib can improve perfusion without affecting tumor angiogenesis.

3.3 Vismodegib treatment alleviates solid and fluid stresses

Subsequently, to further explore the potential of vismodegib to normalize the tumor microenvironment, we performed detailed analysis of the mechanical properties of the tumors. As it has been previously demonstrated, improved perfusion is achieved by alleviation of intratumoral solid stresses [7–9]. Furthermore, reduction of ECM fibers has the potential to alleviate IFP, which can enhance delivery of drugs [1]. Therefore, we carried out experiments to investigate whether vismodegib treatment affects solid stresses and IFP. We performed *ex vivo* stress-strain experiments under compression on vismodegib or control-treated pancreatic tumors (Figure 3A, left), which revealed that the mean values of the elastic modulus were decreased in both tumor types, presumably owing to hyaluronan reduction that resist compressive strains. However, the change in the elastic modulus was statistically significant only for the BxPC3 tumors (Figure 3B). In addition, we examined the effect of vismodegib on tumor fluid phase features and particularly on the interstitial hydraulic conductivity and IFP. To calculate the hydraulic conductivity, we performed *ex vivo* stress-relaxation experiments during which the tumor is rapidly squeezed by two platens and held to a constant compression so that the interstitial fluid will equilibrate, resulting in its partial leakiness from the tumor (Figure 3A, right). Hydraulic conductivity is a measure of the easiness by which interstitial fluid percolates in the tumor ECM and, thus, the higher the conductivity the more fluid will leak from the tumor during compression. The values of the hydraulic conductivity can be extracted from the experiments using mathematical modeling [8, 9]. IFP was measured using the wick-in-needle technique [24]. We found that treatment with vismodegib significantly increased hydraulic conductivity by

approximately 4-fold in both MiaPaCa2 and BxPC3 tumors (Figure 3C) and alleviated IFP by 2.5 and 3-fold, respectively (Figure 3D).

3.4 Vismodegib improves the efficacy of chemotherapy

Based on our results, we hypothesized that vismodegib can improve the efficacy of chemotherapy. To investigate our hypothesis, we performed tumor growth studies in MiaPaCa2 and BxPC3 pancreatic tumors. Mice orally received mock treatment or vismodegib (40 mg/kg) starting 35 days (MiaPaCa2) and 4 days (BxPC3) post-implantation of cancer cells, whereas administration of gemcitabine (50 mg/kg, i.p.) begun on day 45 (MiaPaCa2) or day 11 (BxPC3). Tumor volume was measured throughout the treatment period. In our study, we found that vismodegib alone or gemcitabine alone did not influence primary tumor growth (Figure 4). However, combinatorial treatment with vismodegib and gemcitabine dramatically decreased tumor volume in MiaPaCa2 model and significantly delayed tumor growth in BxPC3. A higher dose of vismodegib (100 mg/kg) was also tested in combination with gemcitabine in MiaPaCa2 tumors which resulted in a similar growth effect compared to the lower dose (data not shown). Therefore, targeting the tumor microenvironment with vismodegib significantly improved the therapeutic outcome of standard chemotherapy.

3.5 Vismodegib increases delivery of doxorubicin to tumors but not to normal tissues

To verify that normalization of the tumor microenvironment increases delivery of drugs, we performed biodistribution analysis in MiaPaCa2 tumors, following the same treatment protocol as in the previous experiments. More specifically, 20 mg/kg of doxorubicin was injected intravenously (i.v.) to animals 4 hours prior to sacrifice. Doxorubicin concentration in tissue sample homogenates was determined by quantification of fluorescence intensity and calculated based on a standard curve generated by addition and measurement of known amounts of doxorubicin to normal tissue homogenates of non-treated animals. Our data indicate that there was a significant 2-fold increase in doxorubicin concentration in vismodegib-treated tumors compared to the control group, whereas there was no effect in the delivery of the drug to any normal tissue tested, including heart, liver or kidney (Figure 5).

3.6 Vismodegib inhibits Sonic hedgehog signaling in stromal cells

Based on previous studies suggesting that vismodegib exerts its effects by suppressing the SHH signaling pathway in CAFs [11], we wanted to investigate and confirm potential gene expression changes in our *in vivo* tumor models. To this end, we performed real-time PCR analysis for the expression of selected genes in both MiaPaCa2 and BxPC3 tumors. We found that while vismodegib was able to suppress the expression of the two major SHH pathway downstream effector genes, Gli1 and Gli2, in stromal genes it had no effect on the expression of these genes in human MiaPaCa2 cancer cells (Figure 6). Similar stromal-specific effects were also observed for Gli1 expression in BxPC3 tumors (Supplementary Figure S4). This evidence collectively suggests that vismodegib is able to remodel the pancreatic tumor microenvironment primarily by targeting SHH signaling in host stromal cells which, in large part, are comprised by CAFs.

3.7 Vismodegib improves the efficacy of Abraxane and Doxil

Finally, we wanted to extend our analysis to other desmoplastic tumors as well to test the ability of vismodegib to also enhance the efficacy of common cancer nanomedicines. To this end, we employed an orthotopic breast xenograft tumor model, using human MCF10CA1a breast cancer cells implanted in the mammary fat pad of CD1 nude mice and investigated the effect of vismodegib on the efficacy of the most common nanomedicines used for the treatment of breast cancer, Abraxane and Doxil. Abraxane is a 130 nm albumin-bound paclitaxel that shrinks to 10nm following dilution to plasma [21] and Doxil is an 100nm pegylated liposomal doxorubicin. In this model, mice orally received mock treatment or vismodegib 4 days post-implantation of cancer cells, whereas administration of nanoparticles begun on day 14 and tumor volume was measured throughout the treatment period. We found that vismodegib, Doxil (3 mg/kg, i.v.) or Abraxane (20 mg/kg, i.v.) alone did not influence primary tumor growth (Figure 7). On the other hand, combined administration of vismodegib and Abraxane significantly delayed tumor growth compared to Abraxane alone. Similarly, combination of Doxil and vismodegib significantly reduced tumor volume compared to monotherapy (Figure 7). Consistent with our previous findings in pancreatic tumor models, vismodegib also decreased IFP and the elastic modulus of breast tumors (Supplementary Figure S5).

4 Discussion

In the current study, we aimed to investigate the effect of targeting CAFs in the efficacy of chemo-and nanotherapeutic drugs, using the SHH pathway inhibitor vismodegib, in different xenograft mouse models of desmoplastic pancreatic and breast cancers. Our data indicate that vismodegib primarily targets CAFs by inhibiting their proliferation rate. This effect appears to be mediated by suppression of the SHH signaling pathway, as evident by downregulation of Gli1 and Gli2 gene expression, in stromal but not human pancreatic cancer cells in our xenograft mouse models. These data are consistent with previous studies suggesting that vismodegib is an effective inhibitor of the SHH pathway in stromal cells and acts to suppress the functionality of CAFs in pancreatic cancers [11]. Our data presented here extend previous findings and show that depletion of CAFs has profound effects in remodeling of the tumor microenvironment, thus promoting solid and fluid stress alleviation in vismodegib-treated pancreatic and breast tumors, which enhances drug delivery and significantly improves the efficacy of chemotherapy and common nanomedicines. Our findings suggest that this is mediated by both the elimination of CAFs from the tumor mass as well as by reduction in the amount of ECM components which, in large part, are produced by the CAFs [34, 35].

Most importantly, and despite the fact that recent clinical trials have failed to show that combining vismodegib with gemcitabine can cause significant enhancement in treatment efficacy and overall survival in patients with metastatic pancreatic cancer [13], our novel findings suggest that similar studies could be worth revisiting in a more targeted group of patients with highly desmoplastic, fibroblast-rich tumors, rather than in unselected cohorts. Furthermore, our data using orthotopic xenograft models for human breast cancer strongly suggest that vismodegib-induced depletion of CAFs and remodeling of the ECM can also

dramatically enhance the efficacy of clinically approved nanomedicines of various sizes, such as Abraxane and Doxil, which are known to have significantly less adverse effects compared to traditional chemotherapies. Similar enhancement in the efficacy of nanotherapy in breast cancer have recently been shown by other stress alleviating agents, such as the TGFβ pathway inhibitors tranilast and pirfenidone as well as the angiotensin II receptor blocker losartan [8, 9, 22].

Therefore, our data collectively suggest that vismodegib-induced CAFs depletion normalizes the microenvironment of desmoplastic tumors and induces alleviation of intratumoral stresses, increasing blood vessel perfusion and drug delivery. Since vismodegib has been already approved for clinical use, it could be combined with common chemo- and nanotherapeutic drugs in selected patients with desmoplastic pancreatic and breast cancers to significantly improve treatment efficacy and overall survival. We suggest that such findings could directly lead to Phase II clinical trials in targeted groups of patients to test the efficacy of this therapeutic strategy in humans. Finally, anti-fibrotic drugs such as losartan, tranilast and pirfenidone have been also used successfully to normalize the desmoplastic tumor micro-environment by targeting the tumor ECM [7–9]. Here, we showed that direct targeting of CAFs can cause an indirect decrease in ECM content, suggesting that vismodegib can modulate both components of tumor stroma.

Supplementary Material

Refer to Web version on PubMed Central for supplementary material.

Acknowledgments

This work has received funding from the European Research Council under the European Union's Seventh Framework Programme (FP7/2007–2013)/ERC Grant Agreement No. 336839-ReEngineeringCancer and the European Commission (MSCA-IF-2014-657139 STROMAMECH).

References

[1]. Chauhan VP, Stylianopoulos T, Boucher Y, Jain RK. Delivery of molecular and nanomedicine to tumors: Transport barriers and strategies. Annual Reviews Chemical and Biomolecular Engineering. 2011; 2:281–298.

[2]. Jain RK, Martin JD, Stylianopoulos T. The role of mechanical forces in tumor growth and therapy. Annu Rev Biomed Eng. 2014; 16:321–346. [PubMed: 25014786]

[3]. Stylianopoulos T, Martin JD, Chauhan VP, Jain SR, Diop-Frimpong B, Bardeesy N, Smith BL, Ferrone CR, Hornicek FJ, Boucher Y, Munn LL, et al. Causes, consequences, and remedies for growth-induced solid stress in murine and human tumors. Proceedings of the National Academy of Sciences of the United States of America. 2012; 109:15101–15108. [PubMed: 22932871]

[4]. Stylianopoulos T, Martin JD, Snuderl M, Mpekris F, Jain SR, Jain RK. Coevolution of solid stress and interstitial fluid pressure in tumors during progression: Implications for vascular collapse. Cancer research. 2013; 73:3833–3841. [PubMed: 23633490]

[5]. Voutouri C, Polydorou C, Papageorgis P, Gkretsi V, Stylianopoulos T. Hyaluronan-Derived Swelling of Solid Tumors, the Contribution of Collagen and Cancer Cells, and Implications for Cancer Therapy. Neoplasia. 2016; 18:732–741. [PubMed: 27886639]

[6]. Stylianopoulos T. The Solid Mechanics of Cancer and Strategies for Improved Therapy. Journal of biomechanical engineering. 2017; 139

[7]. Chauhan VP, Martin JD, Liu H, Lacorre DA, Jain SR, Kozin SV, Stylianopoulos T, Mousa A, Han X, Adstamongkonkul P, Popovic Z, et al. Angiotensin inhibition enhances drug delivery and

Europe PMC Funders Author Manuscripts

potentiates chemotherapy by decompressing tumor blood vessels. Nature communications. 2013; 4doi: 10.1038/ncomms.3516

[8]. Papageorgis P, Polydorou C, Mpekris F, Voutouri C, Agathokleous E, Kapnissi-Christodoulou CP, Stylianopoulos T. Tranilast-induced stress alleviation in solid tumors improves the efficacy of chemo- and nanotherapeutics in a size-independent manner. Scientific reports. 2017; 7:46140. [PubMed: 28393881]

[9]. Polydorou C, Mpekris F, Papageorgis P, Voutouri C, Stylianopoulos T. Pirfenidone normalizes the tumor microenvironment to improve chemotherapy. Oncotarget. 2017; 8:24506–24517. [PubMed: 28445938]

[10]. Murphy JE, Wo JYL, Ferrone C, Jiang W, Yeap BY, Blaszkowsky LS, Kwak EL, Allen JN, Clark JW, Faris JE, Zhu AX, et al. TGF-B1 inhibition with losartan in combination with FOLFIRINOX (F-NOX) in locally advanced pancreatic cancer (LAPC): Preliminary feasibility and R0 resection rates from a prospective phase II study. J Clin Oncol. 2017; 35 (suppl 4S; abstract 386).

[11]. Olive KP, Jacobetz MA, Davidson CJ, Gopinathan A, McIntyre D, Honess D, Madhu B, Goldgraben MA, Caldwell ME, Allard D, Frese KK, et al. Inhibition of Hedgehog signaling enhances delivery of chemotherapy in a mouse model of pancreatic cancer. Science. 2009; 324:1457–1461. [PubMed: 19460966]

[12]. Madden, JI. Infinity reports update from phase 2 study of saridegib plus gemcitabine in patients with metastatic pancreatic cancer. http://www.businesswire.com/news/home/20120127005146/en/Infinity-Reports-Update-Phase-2-Study-Saridegib#.Vg2sAuGJMQM

[13]. Catenacci DV, Junttila MR, Karrison T, Bahary N, Horiba MN, Nattam SR, Marsh R, Wallace J, Kozloff M, Rajdev L, Cohen D, et al. Randomized Phase Ib/II Study of Gemcitabine Plus Placebo or Vismodegib, a Hedgehog Pathway Inhibitor, in Patients With Metastatic Pancreatic Cancer. Journal of clinical oncology : official journal of the American Society of Clinical Oncology. 2015; 33:4284–4292. [PubMed: 26527777]

[14]. Ozdemir BC, Pentcheva-Hoang T, Carstens JL, Zheng X, Wu CC, Simpson TR, Laklai H, Sugimoto H, Kahlert C, Novitskiy SV, De Jesus-Acosta A, et al. Depletion of carcinoma-associated fibroblasts and fibrosis induces immunosuppression and accelerates pancreas cancer with reduced survival. Cancer cell. 2014; 25:719–734. [PubMed: 24856586]

[15]. Rhim AD, Oberstein PE, Thomas DH, Mirek ET, Palermo CF, Sastra SA, Dekleva EN, Saunders T, Becerra CP, Tattersall IW, Westphalen CB, et al. Stromal elements act to restrain, rather than support, pancreatic ductal adenocarcinoma. Cancer cell. 2014; 25:735–747. [PubMed: 24856585]

[16]. Lee JJ, Perera RM, Wang H, Wu DC, Liu XS, Han S, Fitamant J, Jones PD, Ghanta KS, Kawano S, Nagle JM, et al. Stromal response to Hedgehog signaling restrains pancreatic cancer progression. Proceedings of the National Academy of Sciences of the United States of America. 2014; 111:E3091–3100. [PubMed: 25024225]

[17]. Jeng KS, Jeng CJ, Jeng WJ, Sheen IS, Chang CF, Hsiau HI, Hung ZH, Yu MC, Chang FY. Sonic hedgehog pathway inhibitor mitigates mouse hepatocellular carcinoma. American journal of surgery. 2015; 210:554–560. [PubMed: 26073903]

[18]. Yauch RL, Dijkgraaf GJ, Alicke B, Januario T, Ahn CP, Holcomb T, Pujara K, Stinson J, Callahan CA, Tang T, Bazan JF, et al. Smoothened mutation confers resistance to a Hedgehog pathway inhibitor in medulloblastoma. Science. 2009; 326:572–574. [PubMed: 19726788]

[19]. Dijkgraaf GJ, Alicke B, Weinmann L, Januario T, West K, Modrusan Z, Burdick D, Goldsmith R, Robarge K, Sutherlin D, Scales SJ, et al. Small molecule inhibition of GDC-0449 refractory smoothened mutants and downstream mechanisms of drug resistance. Cancer research. 2011; 71:435–444. [PubMed: 21123452]

[20]. Papageorgis P, Ozturk S, Lambert AW, Neophytou CM, Tzatsos A, Wong CK, Thiagalingam S, Constantinou AI. Targeting IL13Ralpha2 activates STAT6-TP63 pathway to suppress breast cancer lung metastasis. Breast cancer research : BCR. 2015; 17:98. [PubMed: 26208975]

[21]. Chauhan VP, Stylianopoulos T, Martin JD, Popovic Z, Chen O, Kamoun WS, Bawendi MG, Fukumura D, Jain RK. Normalization of tumour blood vessels improves the delivery of nanomedicines in a size-dependent manner. Nature Nanotechnology. 2012; 7:383–388.

[22]. Diop-Frimpong B, Chauhan VP, Krane S, Boucher Y, Jain RK. Losartan inhibits collagen I synthesis and improves the distribution and efficacy of nanotherapeutics in tumors. Proceedings

of the National Academy of Sciences of the United States of America. 2011; 108:2909–2914. [PubMed: 21282607]

[23]. Volk LD, Flister MJ, Chihade D, Desai N, Trieu V, Ran S. Synergy of nab-paclitaxel and bevacizumab in eradicating large orthotopic breast tumors and preexisting metastases. Neoplasia. 2011; 13:327–338. [PubMed: 21472137]

[24]. Fadnes HO, Reed RK, Aukland K. Interstitial fluid pressure in rats measured with a modified wick technique. Microvascular research. 1977; 14:27–36. [PubMed: 895543]

[25]. Boucher Y, Baxter LT, Jain RK. Interstitial pressure gradients in tissue-isolated and subcutaneous tumors: implications for therapy. Cancer research. 1990; 50:4478–4484. [PubMed: 2369726]

[26]. Laginha KM, Verwoert S, Charrois GJ, Allen TM. Determination of doxorubicin levels in whole tumor and tumor nuclei in murine breast cancer tumors. Clinical cancer research : an official journal of the American Association for Cancer Research. 2005; 11:6944–6949. [PubMed: 16203786]

[27]. Papageorgis P, Lambert AW, Ozturk S, Gao F, Pan H, Manne U, Alekseyev YO, Thiagalingam A, Abdolmaleky HM, Lenburg M, Thiagalingam S. Smad signaling is required to maintain epigenetic silencing during breast cancer progression. Cancer research. 2010; 70:968–978. [PubMed: 20086175]

[28]. Angeli S, Stylianopoulos T. Biphasic modeling of brain tumor biomechanics and response to radiation treatment. Journal of biomechanics. 2016

[29]. Mpekris F, Angeli S, Pirentis AP, Stylianopoulos T. Stress-mediated progression of solid tumors: effect of mechanical stress on tissue oxygenation, cancer cell proliferation, and drug delivery. Biomechanics and modeling in mechanobiology. 2015; 14:1391–1402. [PubMed: 25968141]

[30]. Wong H, Alicke B, West KA, Pacheco P, La H, Januario T, Yauch RL, de Sauvage FJ, Gould SE. Pharmacokinetic-pharmacodynamic analysis of vismodegib in preclinical models of mutational and ligand-dependent Hedgehog pathway activation. Clinical cancer research : an official journal of the American Association for Cancer Research. 2011; 17:4682–4692. [PubMed: 21610148]

[31]. Heyne GW, Melberg CG, Doroodchi P, Parins KF, Kietzman HW, Everson JL, Ansen-Wilson LJ, Lipinski RJ. Definition of critical periods for Hedgehog pathway antagonist-induced holoprosencephaly, cleft lip, and cleft palate. PloS one. 2015; 10:e0120517. [PubMed: 25793997]

[32]. Yue Q, Chen YH, Mulder T, Deese A, Takahashi R, Rudewicz PJ, Reynolds M, Solon E, Hop CE, Wong H, Khojasteh SC. Absorption, distribution, metabolism, and excretion of [(1)(4)C]GDC-0449 (vismodegib), an orally active hedgehog pathway inhibitor, in rats and dogs: a unique metabolic pathway via pyridine ring opening. Drug metabolism and disposition: the biological fate of chemicals. 2011; 39:952–965. [PubMed: 21363998]

[33]. Yang H, Cong WN, Yoon JS, Egan JM. Vismodegib, an antagonist of hedgehog signaling, directly alters taste molecular signaling in taste buds. Cancer medicine. 2015; 4:245–252. [PubMed: 25354792]

[34]. Papageorgis P, Stylianopoulos T. Role of TGFbeta in regulation of the tumor microenvironment and drug delivery (review). International journal of oncology. 2015; 46:933–943. [PubMed: 25573346]

[35]. Gkretsi V, Stylianou A, Papageorgis P, Polydorou C, Stylianopoulos T. Remodeling Components of the Tumor Microenvironment to Enhance Cancer Therapy. Frontiers in oncology. 2015; 5:214. [PubMed: 26528429]

Europe PMC Funders Author Manuscripts

Europe PMC Funders Author Manuscripts

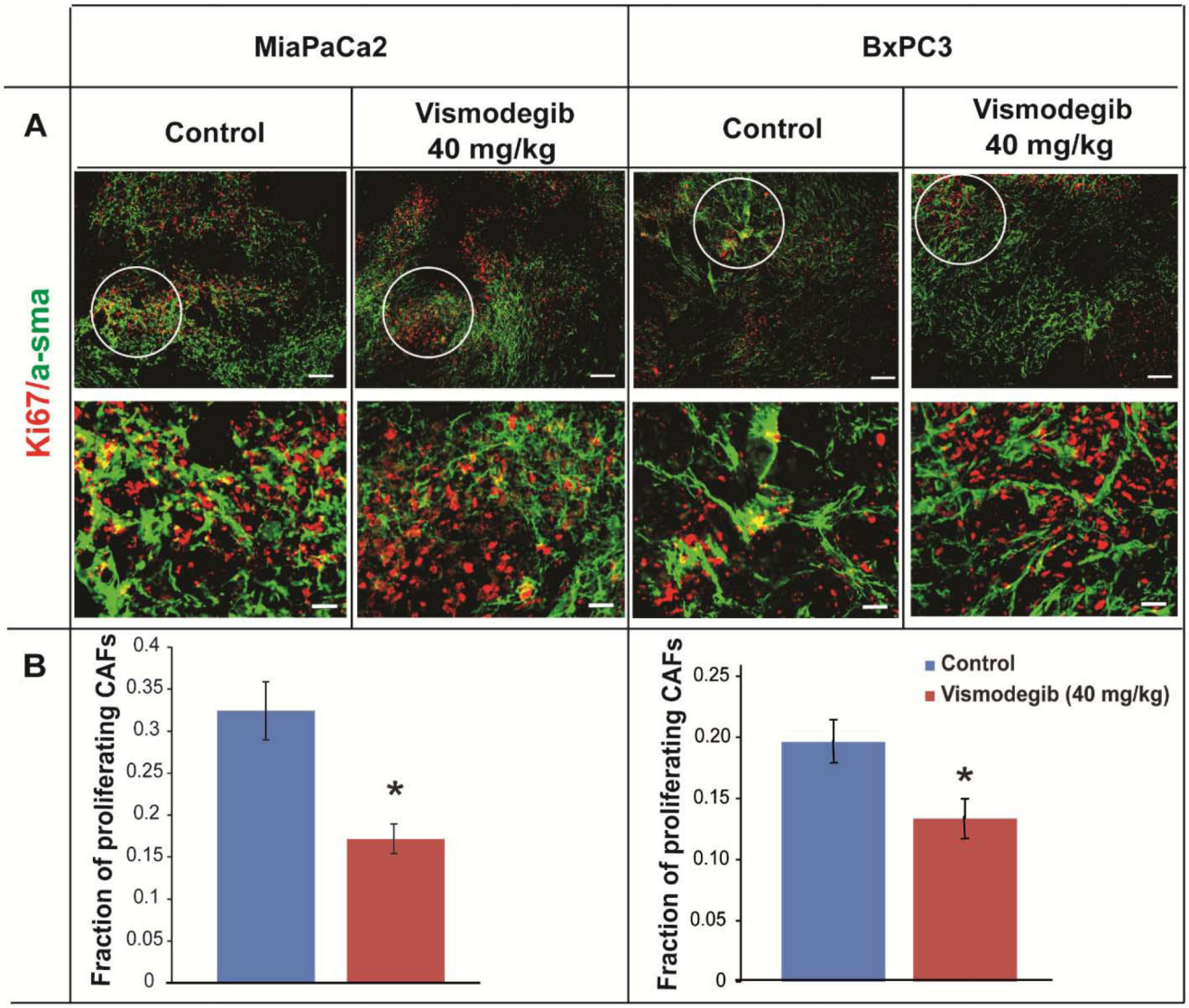

Figure 1. Vismodegib inhibits the activity of cancer-associated fibroblasts in pancreatic tumors.

Representative images from immunofluorescence analysis of MiaPaCa2 or BxPC3 tumors that were mock or vismodegib-treated (40 mg/kg). (A) Tumor sections were stained for the CAF's marker a-SMA (green) and the proliferation marker Ki67 (red). Magnified images from selected tumor areas indicate the presence of Ki67+/a-SMA (yellow) cells. (B) Quantification of Ki67+/a-SMA (yellow) tumor area fraction in MiaPaCa2 or BxPC3 control or vismodegib-treated tumors (n=8-10). Asterisks indicate statistically significant difference between compared groups ($p<0.05$). Scale bar: 25 μm.

Europe PMC Funders Author Manuscripts

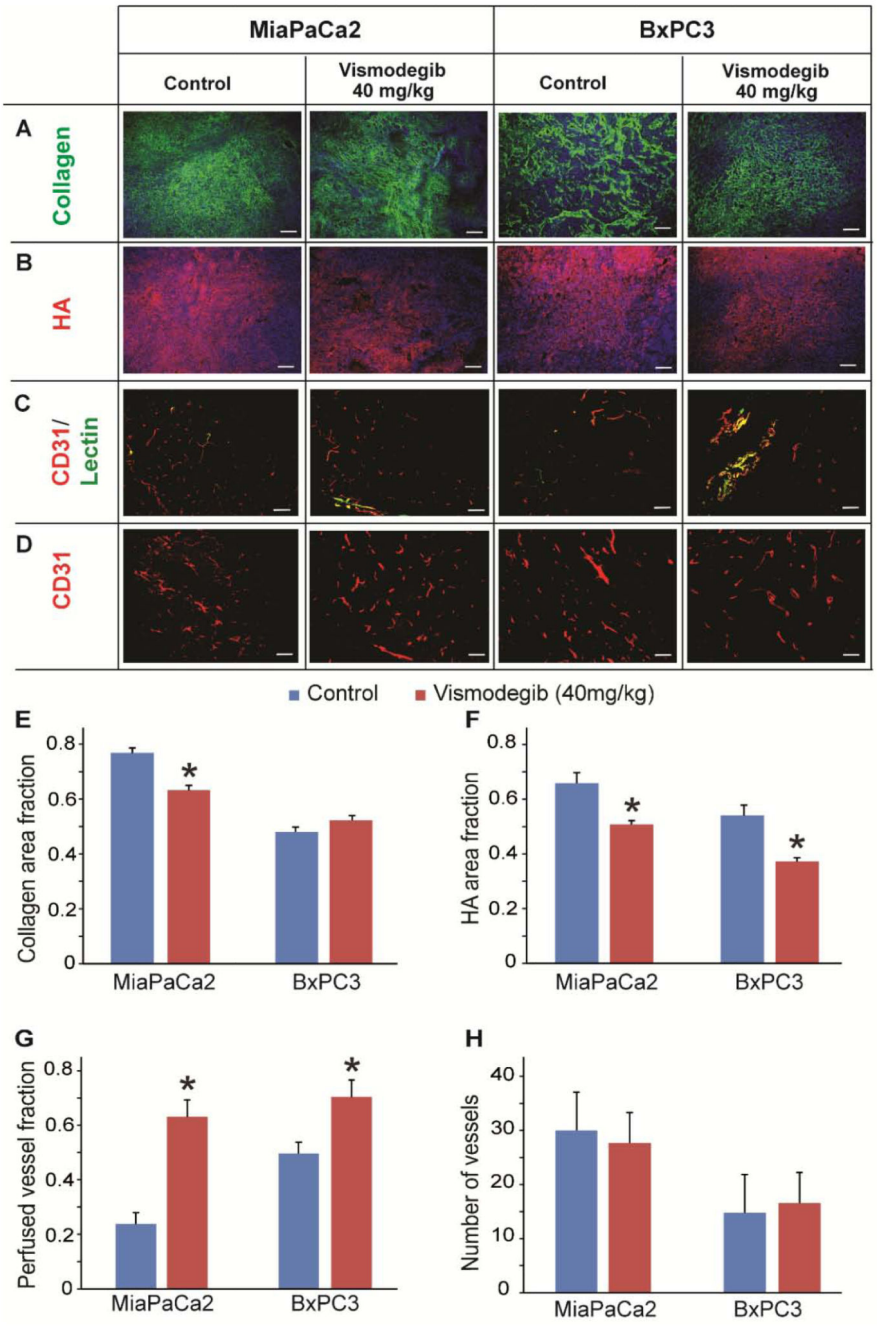

Figure 2. Remodeling of tumor microenvironment using vismodegib.

Representative images from immunofluorescence staining showing the effect of vismodegib (40 mg/kg) on (A) collagen (green) and (B) hyaluronan (HA, red), (C) CD31/Lectin and (D) CD31 levels compared to control-treated MiaPaCa2 or BxPC3 tumors. Quantification of collagen (E) area fractions were found to be significantly lower in vismodegib-treated compared to control-treated MiaPaCa2 tumors ($p = 0.0001$), whereas in BxPC3 tumors no significant changes were observed. Quantification of hyaluronan (F) area fractions were found to be significantly lower in both vismodegib-treated MiaPaCa2 and BxPC3 tumors (p

= 0.02 and p = 3E-5, respectively), compared to control-treated tumors. For both vismodegib-treated pancreatic tumors the fraction of perfused vessels (G) increased compared to control tumors (p = 0.03, MiaPaCa2; p = 0.03, BxPC3). In contrast, quantification of CD31+ area (H) showed no significant change between the groups. Asterisks indicate statistically significant difference between compared groups (n = 8-10). Scale bar: 100 μm.

Europe PMC Funders Author Manuscripts

Europe PMC Funders Author Manuscripts

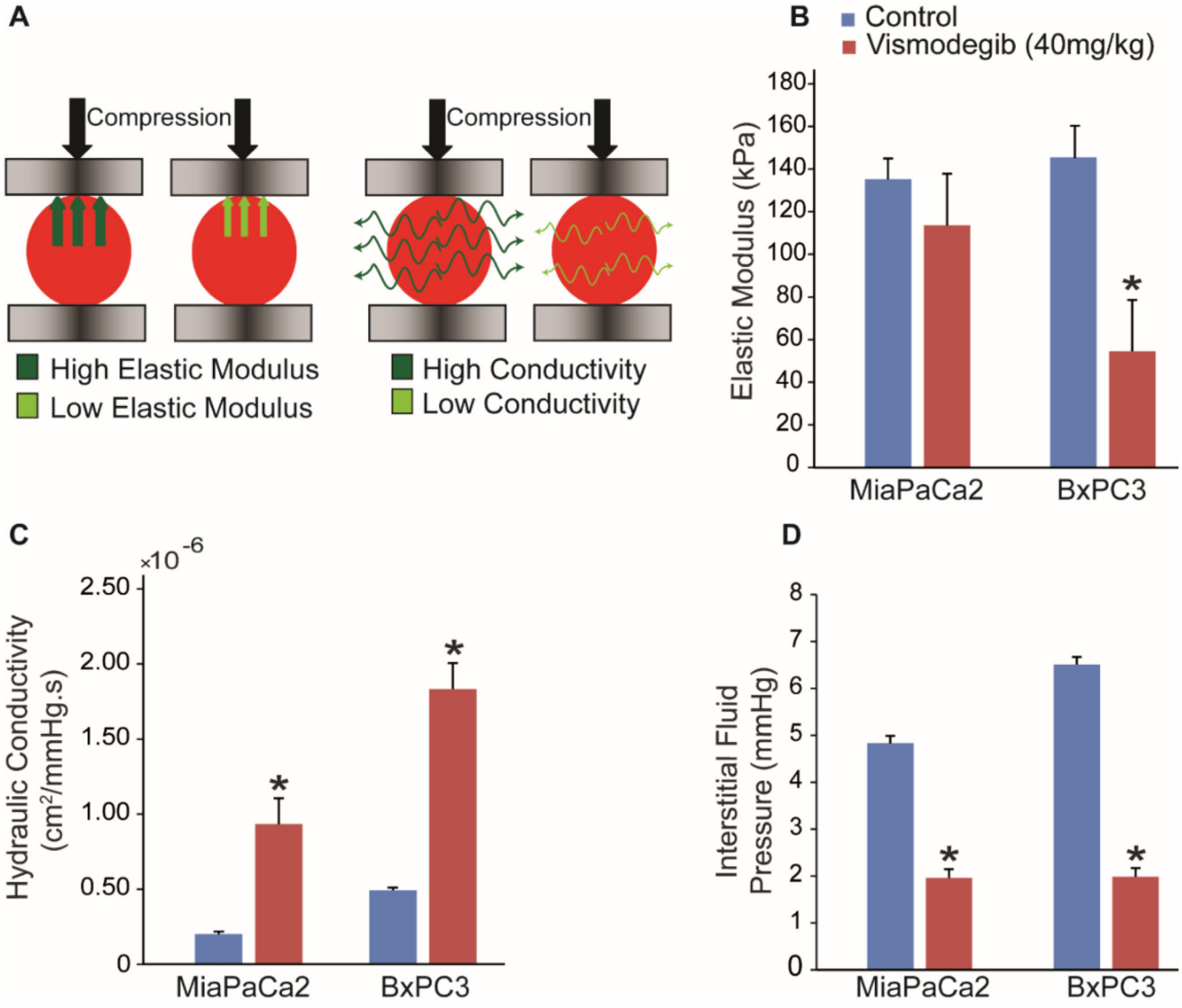

Figure 3. Vismodegib acts as a stress-alleviating agent.

(A) Schematic of the unconfined compression experiment. Desmoplastic tumors become stiff as they grow, exhibiting a higher elastic modulus and resisting stronger to compression. Desmoplasia reduces tumors hydraulic conductivity, resisting to fluid flow through their mass and thus, less fluid exits the tissue during compression. (B) Vismodegib-treated tumors in BxPC3 decreased the elastic modulus compared to control treatment ($p = 0.002$) whereas in MiaPaCa2 had no effect. Vismodegib-induced reduction in ECM content resulted in lower values of hydraulic conductivity of the tumor interstitial space ($p = 0.005$ for MiaPaCa2 and $p = 0.04$ for BxPC3) (C), which in turn caused alleviation of the interstitial fluid pressure ($p = 4E\text{-}9$ for MiaPaCa2 and $p = 5E\text{-}5$ for BxPC3) (D). Asterisks indicate statistically significant difference between compared groups ($n = 8\text{-}10$).

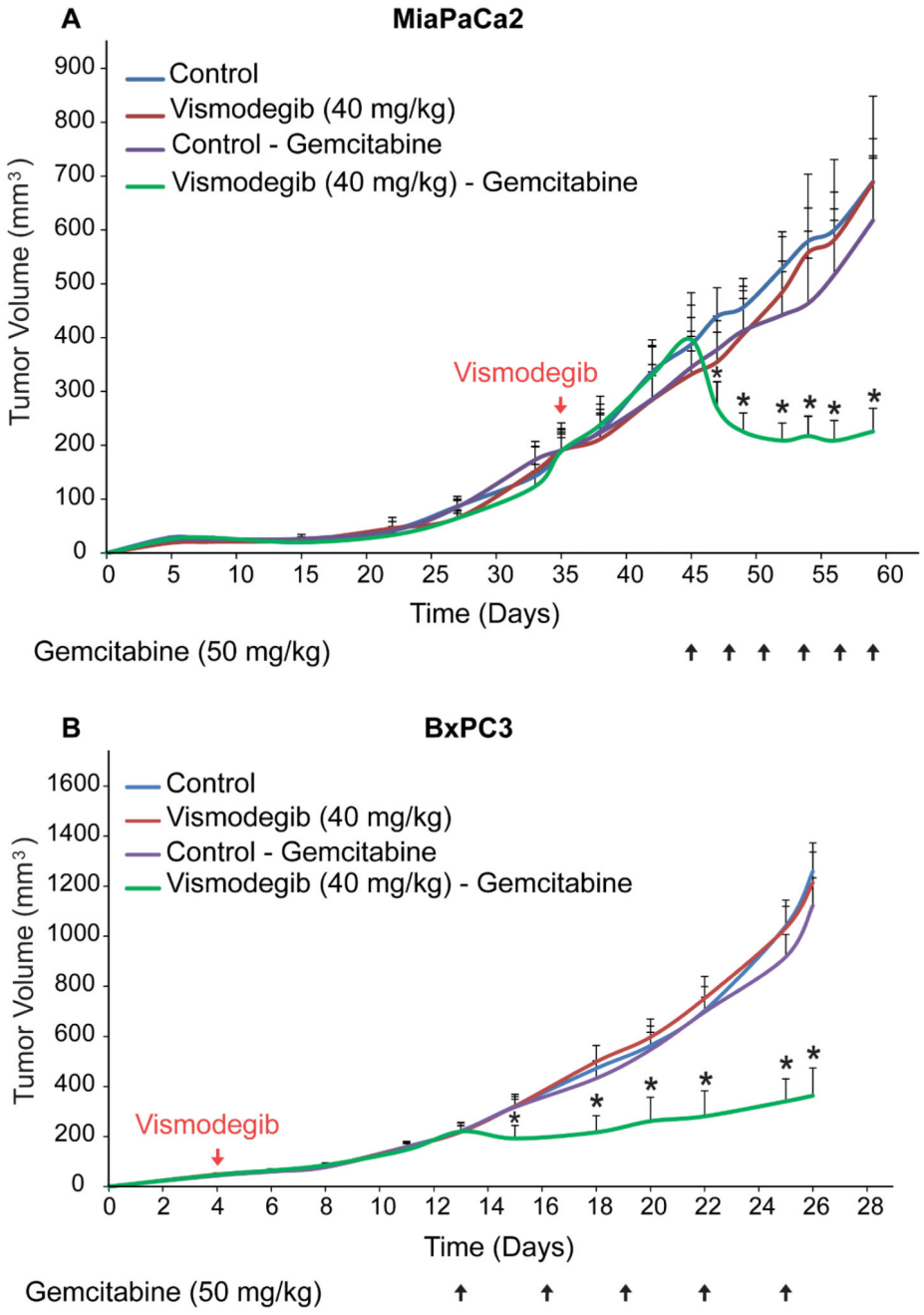

Figure 4. Vismodegib increases anti-tumor efficacy of chemotherapy.

Tumor volume growth rates of (A) MiaPaCa2 and (B) BxPC3 pancreatic human tumors implanted in male NOD/SCID mice. Control treatment (MCT -0.5% methylcellulose, 0.2% Tween 80), vismodegib (40 mg/kg) or gemcitabine (50 mg/kg) alone had no effect on tumor growth in both pancreatic cancer cell lines. (A) Combination of vismodegib and gemcitabine significantly decreased tumor growth of MiaPaCa2 pancreatic tumors compared to gemcitabine monotherapy ($p = 0.005$ on day 60, $n = 8$-10). (B) In BxPC3 model combination of vismodegib and gemcitabine significantly delayed tumor growth compared

to gemcitabine monotherapy ($p = 7E-7$ on day 26, $n = 8-10$). Asterisks indicate a statistically significant difference between compared groups ($p < 0.05$).

Europe PMC Funders Author Manuscripts

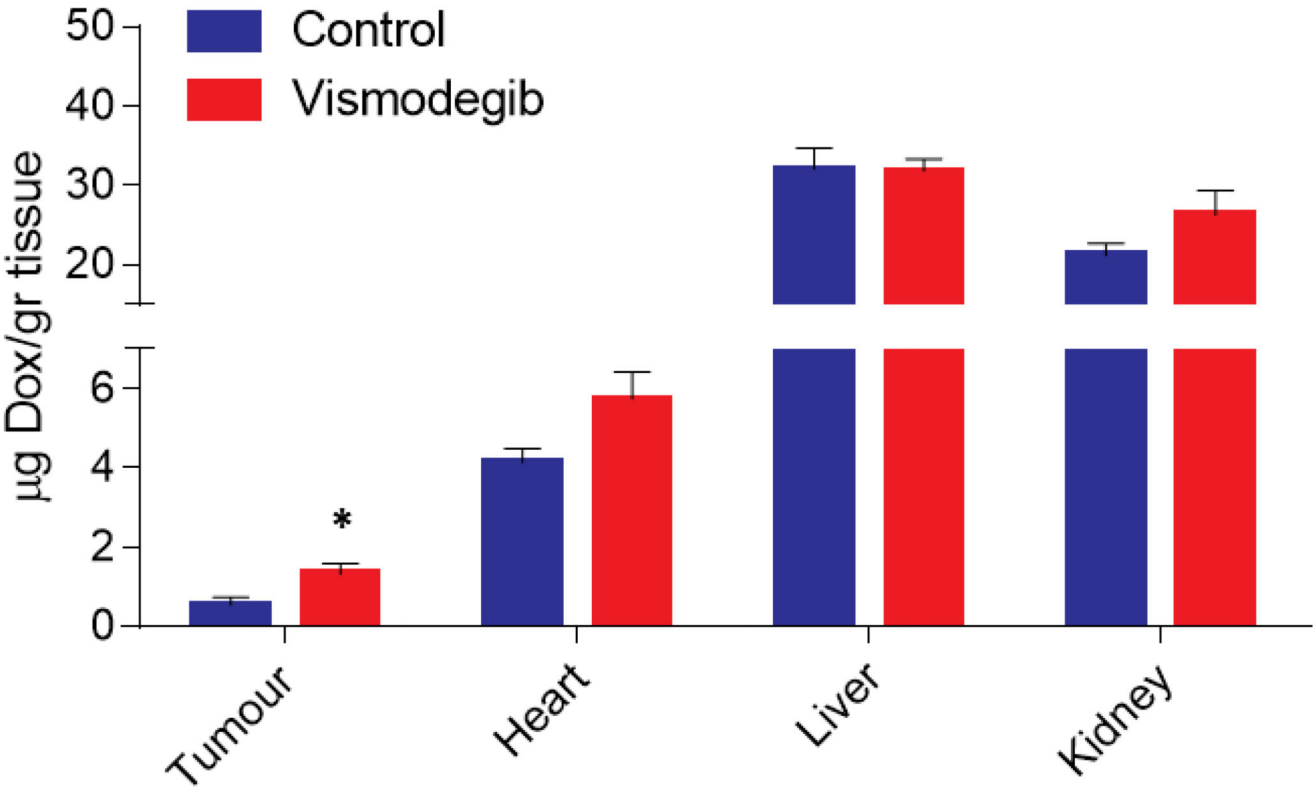

Figure 5. Vismodegib increases intratumoral delivery of doxorubicin.

Quantification of doxorubicin (Dox) concentration in control and vismodegib-treated MiaPaCa2 pancreatic tumors as well as in kidney, liver and heart tissues. Doxorubicin (20 mg/kg) was injected intravenously to the animals 4 hours prior to sacrifice. Vismodegib increased the delivery of doxorubicin by 2-fold in vismodegib-treated compared to control-treated tumors ($p < 0.05$, $n = 9$). No significant differences were observed in drug delivery to normal tissues. Asterisk indicates statistically significant differences between compared groups ($p < 0.05$).

Europe PMC Funders Author Manuscripts

Europe PMC Funders Author Manuscripts

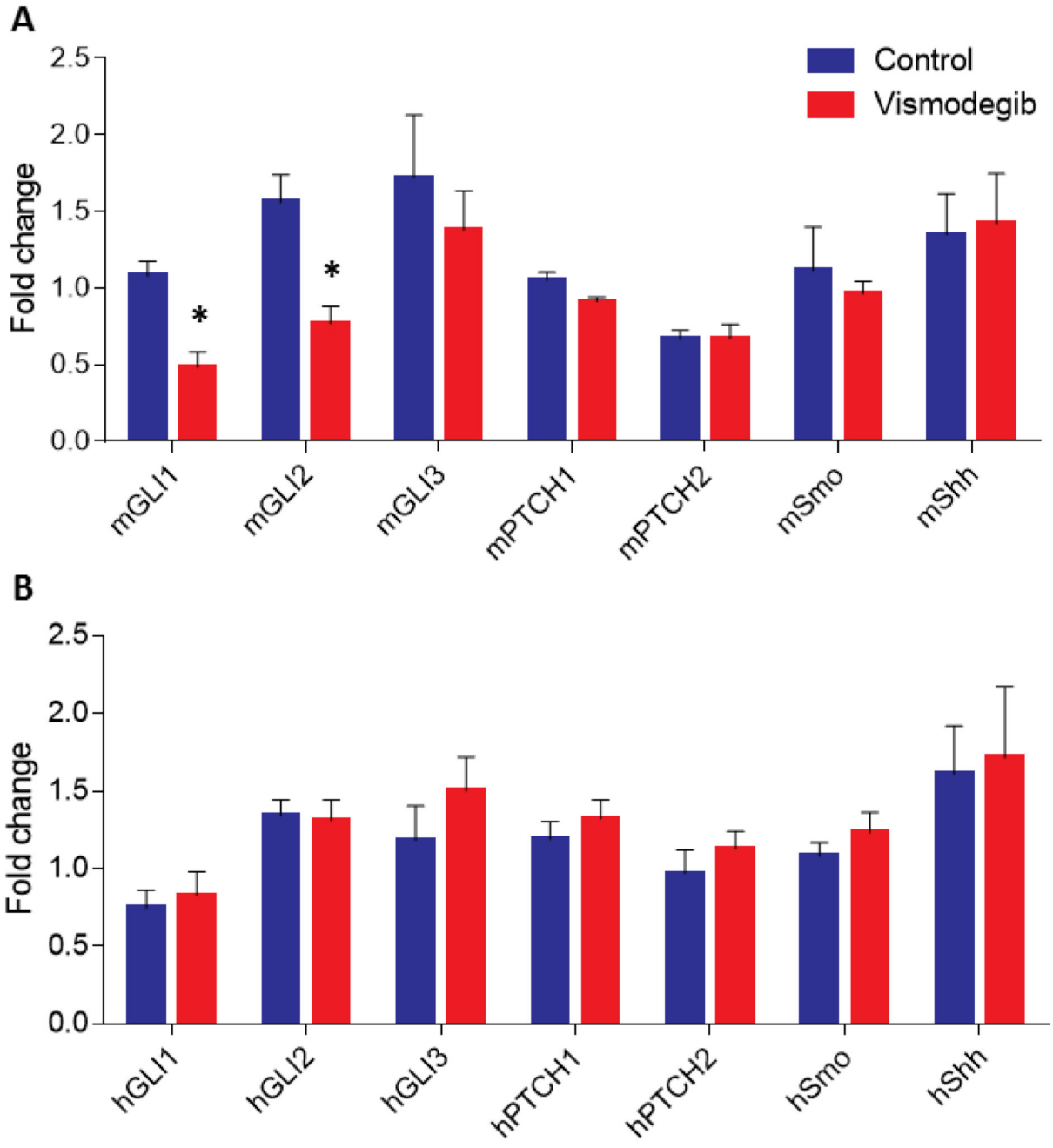

Figure 6. Vismodegib suppresses Sonic hedgehog signaling in stromal cells *in vivo*.

Real-time PCR gene expression analysis and quantification of mouse (A) or human-specific (B) Gli1, Gli2, Gli3, Ptch1, Ptch2, Smo and Shh mRNA levels extracted from control-treated compared to vismodegib-treated MiaPaCa2 tumors, indicated that vismodegib suppressed Gli1 and Gli2 expression in mouse stromal cells but not in MiaPaCa2 human cancer cells. Relative expression for all genes in both groups was normalized based on the expression of beta-actin. Data represent the average of at least 3 independent experiments from 4 control

and 4 vismodegib-treated tumors ± S.E. values and asterisks indicate statistically significant differences between compared groups ($p < 0.05$).

Europe PMC Funders Author Manuscripts

Europe PMC Funders Author Manuscripts

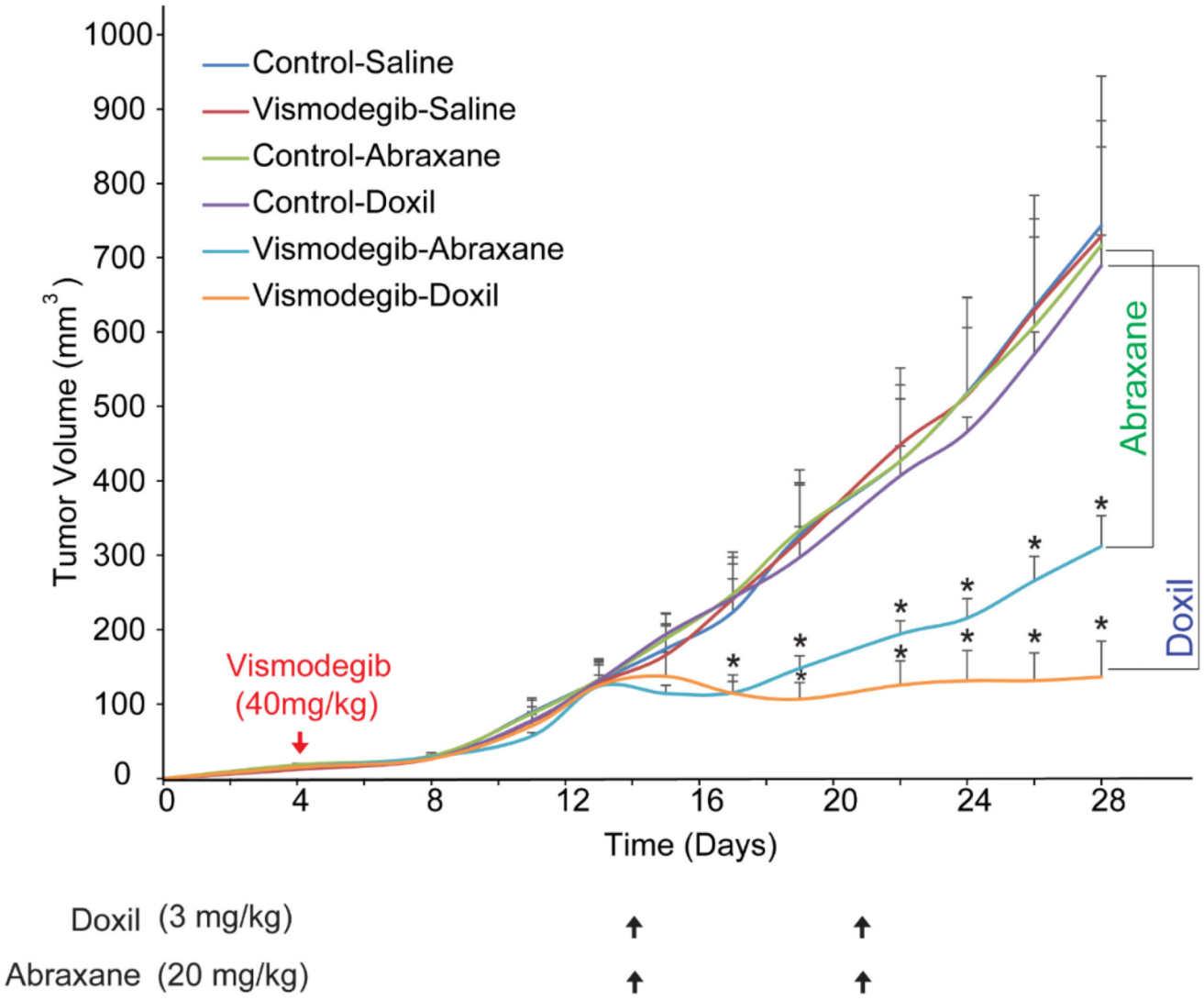

Figure 7. Vismodegib improves anti-tumor efficacy of nanotherapeutics.

Tumor volume growth rates of orthotopic MCF10CA1a breast tumors implanted in CD1 nude mice that were either mock-treated (0.9% NaCl for Abraxane, saline for Doxil and MCT-0.5% methylcellulose, 0.2% Tween 80- for vismodegib), vismodegib-treated alone (40 mg/kg daily *via* gavage), Doxil alone (3 mg/kg on days 14 and 21 post-implantation, i.v.), Abraxane alone (20 mg/kg on days 14 and 21 post-implantation, i.v.), or vismodegib in combination with either Doxil or Abraxane, as described above. Abraxane alone had no effect on tumor volume, compared to combined administration of vismodegib and Abraxane, which significantly delayed tumor growth ($p = 0.02$ on day 28, $n = 6$-8). Additionally, whereas Doxil (3mg/kg) monotherapy had no effect, combination of vismodegib and Doxil significantly decreased tumor volume ($p = 2E\text{-}6$ on day 28, $n = 6$-8) compared to Doxil alone. Asterisks indicate a statistically significant difference between compared groups ($p < 0.05$).